SPE-208665-MS

Deep Learning Enabled Deblurring of Computed Tomography Images of Porous Media

Khalid Labib Alsamadony, King Fahd University of Petroleum and Minerals, College of Petroleum Engineering & Geosciences; Ertugrul Umut Yildirim, Middle East Technical University, Institute of Applied Mathematics; Guenther Glatz, Umair bin Waheed, and Sherif M. Hanafy, King Fahd University of Petroleum and Minerals, College of Petroleum Engineering & Geosciences

This paper was prepared for presentation at the SPE Symposium: Artificial Intelligence - Towards a Resilient and Efficient Energy Industry held virtually on 18 - 19 Oct 2021.

Abstract

Computed tomography (CT) is an important tool to characterize rock samples allowing quantification of physical properties in 3D and 4D. The accuracy of a property delineated from CT data is strongly correlated with the CT image quality. In general, high-quality, lower noise CT Images mandate greater exposure times. With increasing exposure time, however, more wear is put on the X-Ray tube and longer cooldown periods are required, inevitably limiting the temporal resolution of the particular phenomena under investigation.

In this work, we propose a deep convolutional neural network (DCNN) based approach to improve the quality of images collected during reduced exposure time scans. First, we convolve long exposure time images from medical CT scanner with a blur kernel to mimic the degradation caused because of reduced exposure time scanning. Subsequently, utilizing the high- and low-quality scan stacks, we train a DCNN. The trained network enables us to restore any low-quality scan for which high-quality reference is not available. Furthermore, we investigate several factors affecting the DCNN performance such as the number of training images, transfer learning strategies, and loss functions.

The results indicate that the number of training images is an important factor since the predictive capability of the DCNN improves as the number of training images increases. We illustrate, however, that the requirement for a large training dataset can be reduced by exploiting transfer learning. In addition, training the DCNN on mean squared error (MSE) as a loss function outperforms both mean absolute error (MAE) and Peak signal-to-noise ratio (PSNR) loss functions with respect to image quality metrics.

The presented approach enables the prediction of high-quality images from low exposure CT images. Consequently, this allows for continued scanning without the need for X-Ray tube to cool down, thereby maximizing the temporal resolution. This is of particular value for any core flood experiment seeking to capture the underlying dynamics.

Introduction

The use of digital rock physics (DRP) has grown rapidly as a potential source of information about subsurface reservoir characteristics at the pore scale. Imaging high resolution representation of rock samples is at the heart of DRP. After imaging 3D geometry of the mineral phase and the pore-space of a rock, simulation of physical processes enables the quantification of some important rock properties such as permeability, resistivity, and elastic moduli (Andrae et al., 2013). A state-of-the-art technique to acquire images of pore structures is X-ray micro-computed tomography (CT). It reconstructs a 3D image of a sample from a set of X-ray images of the sample taken at different angles (Wildenschild and Sheppard, 2013). For some applications in the oil industry, it is common to use a medical CT scanner, which has a lower resolution than micro-CT. However, for some cases, image resolution of the scanned rock sample should be high enough for the calculation of rock properties effectively. This High resolution (up to few micrometres) can be attained with X-ray micro-computed tomography (micro-CT) (Chung et al., 2019). Therefore, the usage of micro-CT in the area of DRP has increased recently because of its capacity in resolving the porous media internal geometry better than the standard medical CTs.

CT image quality, resolution, and size have a strong effect on the accuracy of the upscaled digital rock property estimation. For example, Bazaikin et al. (2017) showed that the resolution and size of the CT scan need to meet certain conditions for reliable estimation of the effective properties of the Bentheimer sandstone sample. Liu et al. (2018) also demonstrated that there exists a critical resolution for accurately estimating permeability using digital rock analysis. Apart from the resolution, the quality of the scanned rock sample is important. Typical artifacts in CT scans, including noise, blur, streaks, and beam hardening effects cause the quality of the images to decrease. The degraded images require careful processing to allow for meaningful interpretation.

Deep learning (DL) which is a subfield of machine learning (ML) has found many applications in a variety of fields including computer vision. Learning based algorithms have been exploited in CT imaging with applications ranging from medical diagnosis to geosciences. As part of producing high quality images, high resolution images of micro-CT scans for sandstone and carbonate rocks were generated (predicted) from low resolution images using Super Resolution Convolutional Neural Network (SRCNN) (Wang et al., 2019). Furthermore, a low resolution, noisy, blurry image of rock sample can be transformed into super resolution (SR) image with high frequency texture details by combining SRCNN that shows success in capturing edge details with a Generative Adversarial Network (GAN) (Wang et al., 2020). In medical field, low-dose CT is favorable because of the potential radiation risk. Chen et al. (2017) proposed a noise reduction method for degraded low-dose images using a deep convolutional neural network (DCNN).

The objective of this work is to enhance the quality of the blurred CT rock images due to reduced exposure (scan) time by using deep convolutional neural networks (DCNNs). Consequently, this allows for continued scanning without the need for the X-Ray tube to cool down, thereby maximizing the temporal resolution. This is of particular value for any core flood experiment seeking to capture the underlying dynamics. Additionally, we investigate the performance of the network by contrasting various factors like loss function, DCNN architecture, transfer learning, and the size of the training set. The approach is detailed in the method section and the performance evaluation is discussed in the result section.

Method

The training and testing datasets consist of the training examples/labels. These are the high quality (original) CT images that were captured by medical CT scanner using 1 - 4 seconds of exposure time. The low quality (blurred) CT images were created by applying Gaussian blur kernel on the high quality (original) CT images. These low-quality images represent low exposure medical CT images. We train DCNNs to map the low quality/exposure CT images to the high quality/exposure CT images.

The results were generated by training DCNNs on the same training images, from which 64 patches per image of size 41x41 were prepared for training. In all cases, we used the same hyperparameters: Adam optimizer with 0.0001 learning rate, a batch size of 64 and 50 epochs. Additionally, each input image was normalized to be in the range [0 1]. Moreover, DCNNs were trained on residuals. This means that the input is the blurred image, while the output is the residual (the difference between the original image and the blurred image). Then, the predicted residual was added to the blurred image to predict the deblurred image. Residual learning has been suggested by many previous studies to improve DCNN convergence and performance (Kim et al., 2016; Zhang et al., 2017).

We assess the quality of the deblurred image by DCNN using image quality metrics: structural similarity index (SSIM) and peak signal-to-noise ratio (PSNR). For all comparisons, we show the SSIM and PSNR values at different number of training images (50, 100, 150, 200, 250, 300) to see the effect of the number of training images on the DCNN's performance, and to create a more reliable comparison. Thus, each factor can be compared and evaluated at different number of training CT images. All comparisons are done by changing only one factor at a time, to clearly understand the effect of these factors. The deblurred 190 test images by every approach were evaluated quantitatively by SSIM and PSNR using the region of interest (ROI) portion of the high quality (original) images. This means the part of the image that has the rock sample (excluding the core holder).

We investigate the effect of several factors: cropping ROI, loss function, two DCNN architectures and transfer learning using a pre-trained DCNN. The default loss function for training DCNN in MATLAB is the common mean square error (MSE/L2). To change the loss function to mean absolute error (MAE/L1), we followed similar steps as explained in MathWorks (**loss function example**), similarly we implemented PSNR loss function by dividing one over PSNR value of the predicted image during training. MAE loss function minimizes L1 norm of the predicted image, while PSNR loss function maximize the PSNR value of the predicted image.

We compare two DCNN architectures, namely VDSR and U-Net. VDSR has the same architecture as described by Kim et al. (2016). VDSR architecture consists of 20 stacked convolution layers (3x3) and rectified linear units (ReLUs). The other DCNN is based on the U-Net architecture as explained by Ronneberge et al. (2015). This DCNN architecture consists of contracting path (encoder/feature extractor) and expanding path (decoder). The encoder path contains convolution layers (3x3), ReLUs, and max poling (2x2). The decoder part includes convolution layers (3x3), ReLUs, and transposed convolution layers (2x2). U-Net architecture can be created by applying some of the steps presented by Pingel (2019). For applying transfer learning, we obtained the pre-trained VDSR from MathWorks website (super resolution example). The pre-trained weights were obtained by training for the super resolution problem on natural images (Grubinger et al., 2006).

Results

In this section, several configurations are evaluated to provide guidelines on the effect of each of the studied factor. Knowing this would help us obtain the best possible image quality for accurate evaluation of rock samples from CT images without spending additional hours on CT scanning.

The first factor we investigate is cropping the region of interest (ROI). The dimension of each image in the dataset is 512 × 512 pixels, that is the original without cropping. Then, we crop the same ROI from each image, such that each image size is 120 × 120 pixels after cropping. Since the number of patches per image is the same, cropping allows the training image patches to be concentrated in the important area (rock sample). Contrary to that, extracting training patches from the original image (without cropping) reduces the number of image patches that contain the actual rock, and wastes patches of images in the outer region (rock sample holder). Therefore, the advantage of cropping is that it provides image patches with rich features and the most valuable information for training the DCNN. For this reason, the pre-trained VDSR trained on

cropped images is expected to have better performance. This can be observed from both SSIM and PSNR values in Figure 1. Additionally, this benefit is perceived independent of the number of training images compared to the pre-trained VDSR trained on the original images (without cropping). This can be observed by observing the large difference between training the pre-trained VDSR on cropped images and original images (without cropping). This difference is almost the same with the changing number of training images.

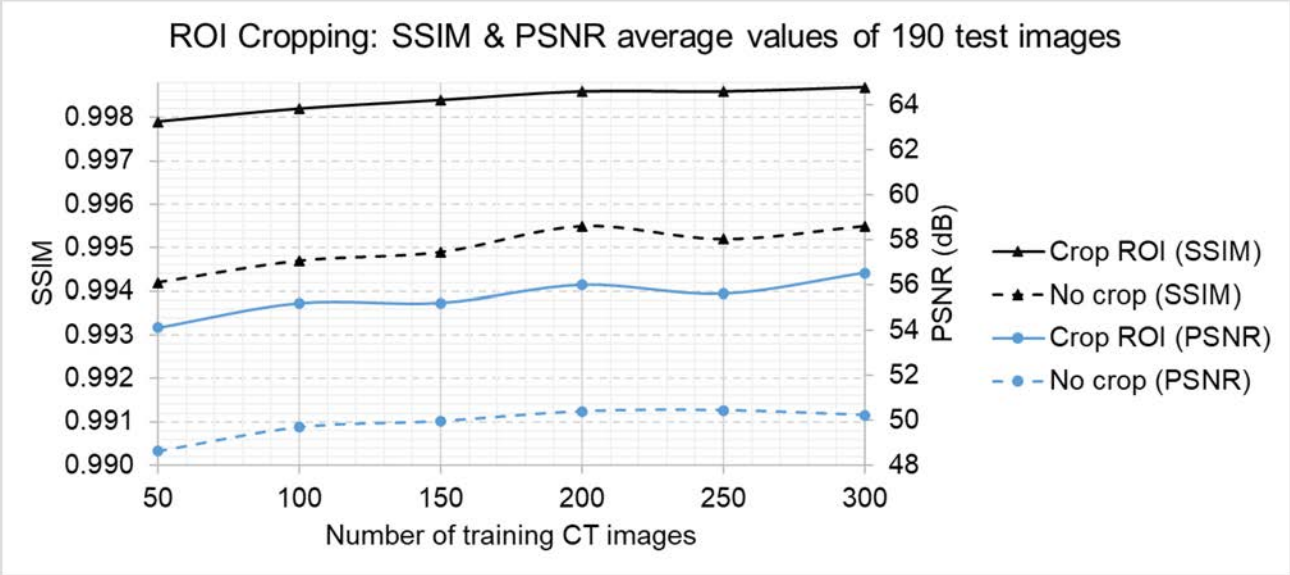

Figure 1—shows the improvement of the pre-trained VDSR results due to cropping ROI.

Loss function may as well impact the training performance of DCNNs (Zhao et al., 2017). We test several loss functions for the pre-trained VDSR to find the optimum loss function for this dataset. L2 loss function (mean square error) results in the best image deblurring quality, followed by PSNR and L1 (mean absolute error) loss functions. Both PSNR and L1 loss functions yield similar deblurring performance. This is based on both SSIM and PSNR values (Figure 2).

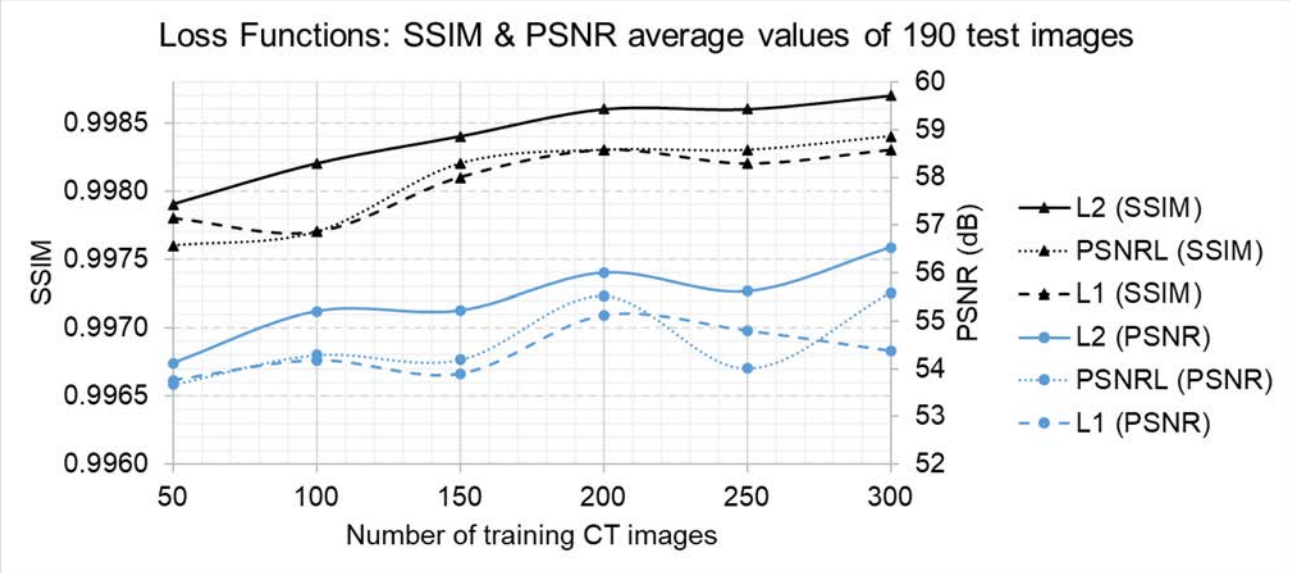

Figure 2—compares the performance of the pre-trained VDSR using different loss functions. PSNRL is PSNR as loss function.

Furthermore, the architecture of DCNN may have a bearing on the clarity of the restored images. In our results, there are two DCNNs: VDSR, which is a deeper (more layers) network with layers stacked sequentially, and the other one is based on U-Net (encoder-decoder). SSIM and PSNR values (Figure 3) indicate that there is no advantage of using a deeper CNN (VDSR) for this dataset, because both DCNNs have comparable results. On the contrary, the U-Net architecture shows better performance on a small number of training images (50 & 100), and therefore may be considered as more efficient.

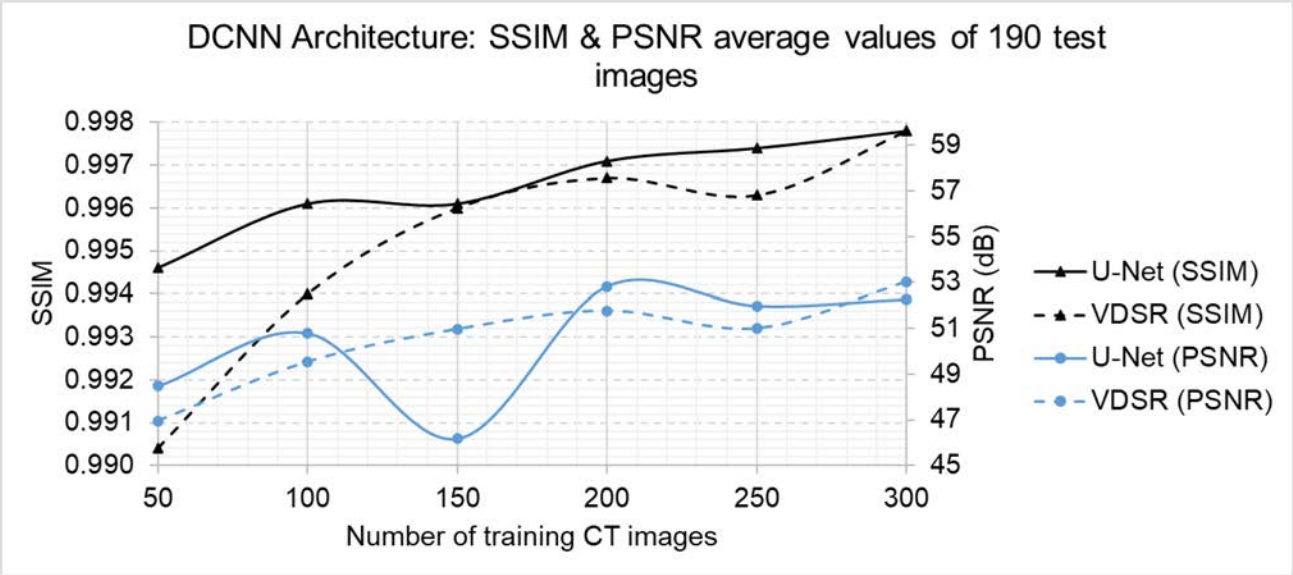

Figure 3—compares two different DCNN architectures: VDSR and U-Net.

Transfer learning can reduce the training time needed to have an adequate performance by utilizing a pre-trained DCNN. The pre-trained VDSR (super resolution example) is compared to VDSR which was trained from scratch and initialized using the method of He et al. (2015). Although the pre-trained VDSR was trained on completely different type of images (e.g., landscapes) and different image restoration task (super resolution), it enhances the restored CT image quality in comparison to training VDSR from scratch (Figure 4). An additional advantage of transfer learning is that it reduces the number of training images needed to get acceptable results. This is clear by observing the significant difference between the pre-trained VDSR and VDSR in SSIM and PSNR values, particularly when using only 50 CT images for training. However, as the number of training images increases, the advantage of transfer learning begins to diminish.

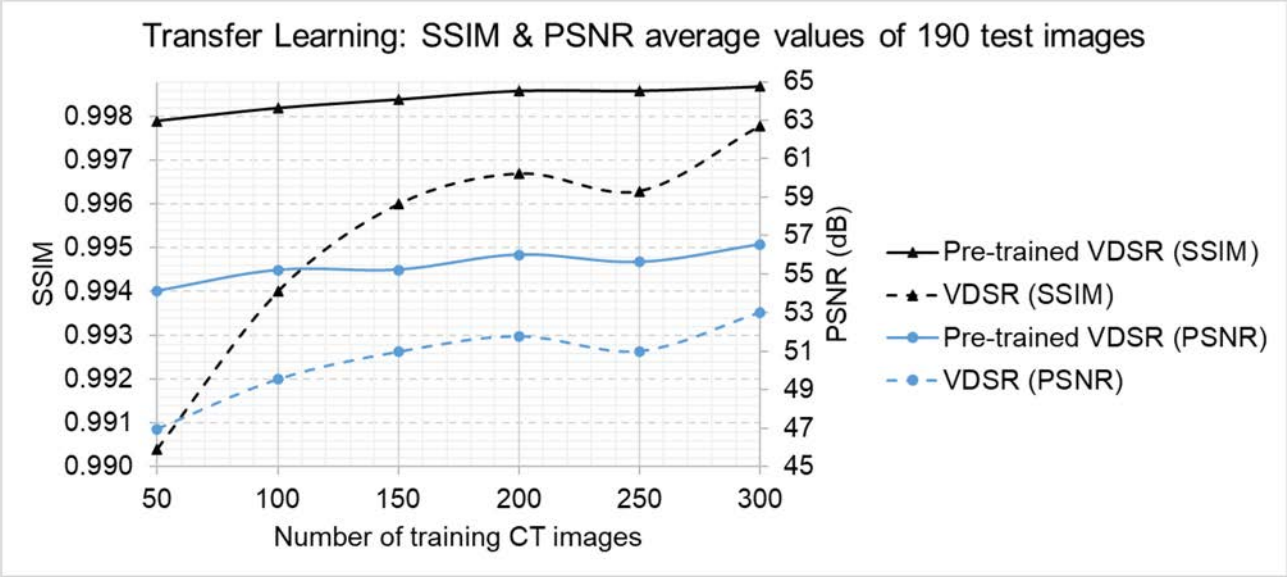

Figure 4—highlights the advantage of transfer learning.

To summarize, the pre-trained VDSR trained on cropped images, 300 training images, and L2 loss function results in the highest SSIM and PSNR values of the test images. The average SSIM and PSNR values of the 190 test images increase from 0.9688 to 0.9987 and from 34 dB to 56.5 dB, respectively. Furthermore, a qualitative assessment (Figure 5 and 6) confirms these high SSIM and PSNR values, where the deblurred test image has minimal errors compared to the pristine image.

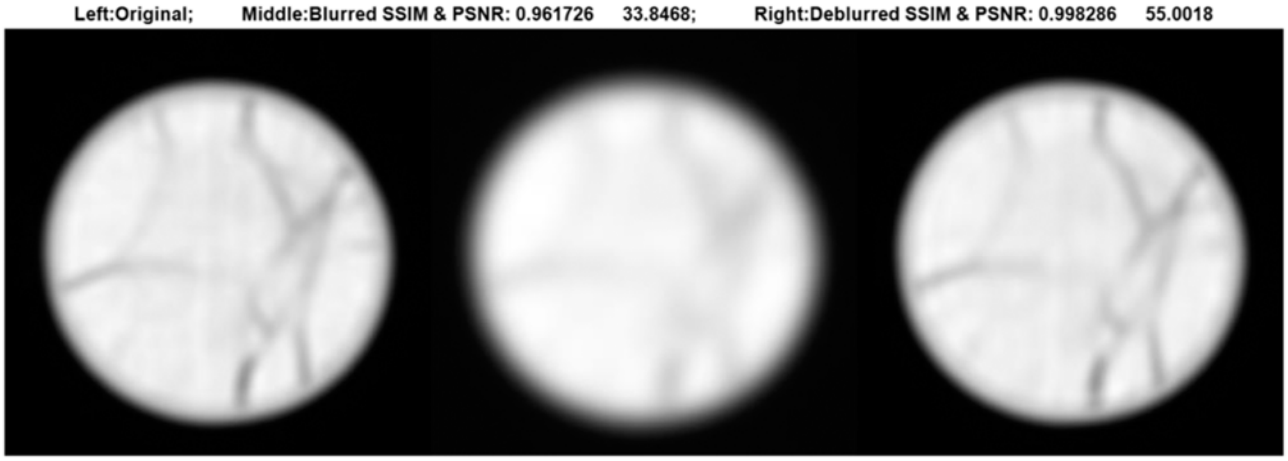

Figure 5—is the qualitive assessment of the pre-trained VDSR trained on 300 cropped CT images and L2 loss function. From left to right, high quality (original), Blurred image (SSIM=0.962, PSNR=33.85 dB), and deblurred image by the pre-trained VDSR (SSIM=0.998, PSNR=55 dB). The three images are on the same scale [0 1].

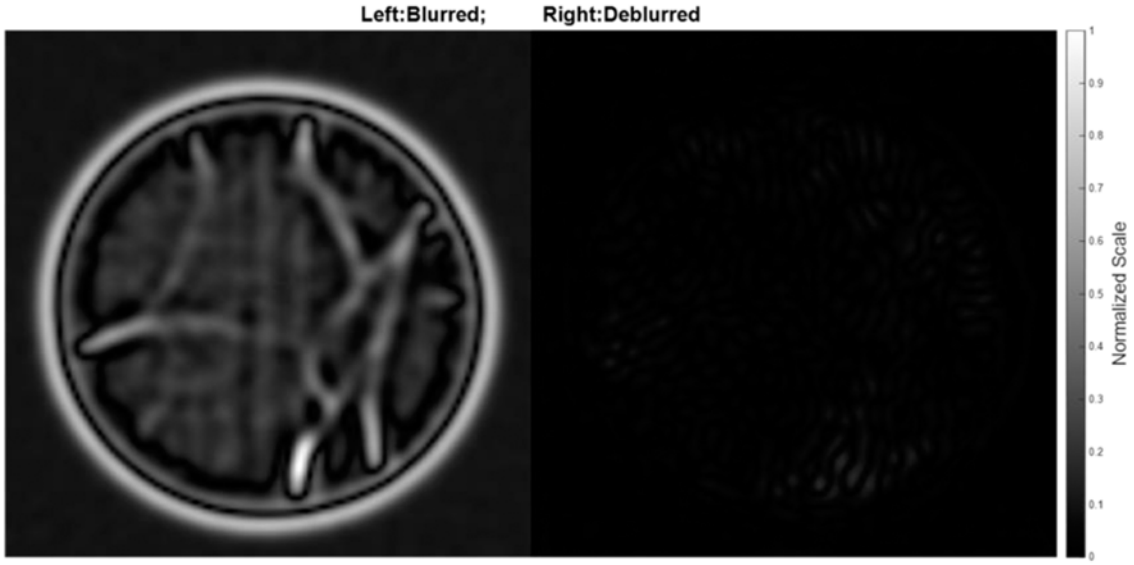

Figure 6—normalized absolute difference between high quality (original) image & blurred image (left). Normalized absolute difference between high quality (original) image & deblurred image (right). The scale of the two images is normalized between 0 and 1.

These results demonstrate that the proposed method can significantly improve artificially blurred medical CT images. Importantly, we have proven the effectiveness of this approach for a noisy micro-CT dataset. Figure 7 exemplifies results where reduced exposure time micro-CT scans of a carbonate rock sample were recovered. The SSIM and PSNR values increased from 0.54 and 23 dB to 0.78 and 34 dB, respectively. Details are provided elsewhere (Alsamadony et al., 2021).

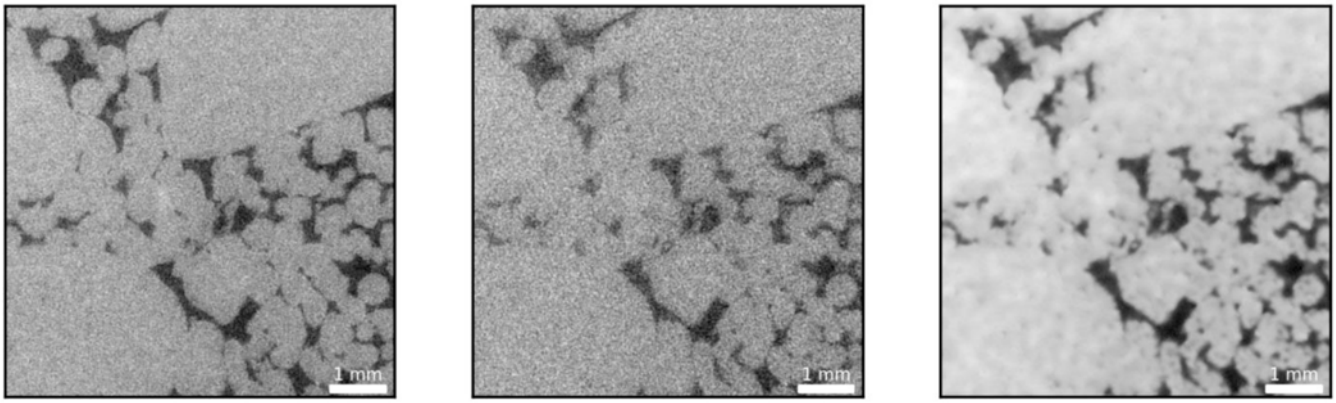

Figure 7—shows the potential of the proposed method for real noisy micro-CT images. From left to right: high exposure image, low exposure image (SSIM = 0.54, PSNR = 23 dB) and the recovered image by VDSR (SSIM = 0.78, PSNR = 34 dB). (Alsamadony et al., 2021).

Conclusion

The goal of this work was to deblur rock CT images by DCNN. This was achieved by experimenting with various factors that might affect the deblurring quality. The factors are cropping ROI, loss function type, the architecture of DCNN and transfer learning. The two factors that have contributed to improving the DCNN deblurring performance were cropping ROI and transfer learning. Remarkably, the deeper DCNN (VDSR) has a comparable performance to the U-Net, and L2 loss function outperforms PSNR and L1 loss functions.

Based on these results, we recommend the following ideas to achieve better deblurring performance using DCNNs. First, to utilize a pre-trained DCNN, even if it was pre-trained on a different type of image restoration task and images. However, using a DCNN that was trained on similar images (CT) and tasks

(e.g., deblurring) might result in more profound improvements. Secondly, cropping irrelevant part of images is suggested as a preprocessing step, since it can vastly enrich the training dataset. These practices would result in clear restored CT images, thus saving hours of lab measurements without compromising reliable analysis and evaluation of rock samples.

References

Alsamadony, K. L., Yildirim, E. U., Glatz, G., Waheed, U. B., & Hanafy, S. M. (2021). Deep Learning Driven Noise Reduction for Reduced Flux Computed Tomography. *Sensors*, **21**(5), 1921. https://doi.org/10.3390/s21051921

Andrä, H., Combaret, N., Dvorkin, J., Glatt, E., Han, J., Kabel, M., Keehm, Y., Krzikalla, F., Lee, M., Madonna, C., Marsh, M., Mukerji, T., Saenger, E. H., Sain, R., Saxena, N., Ricker, S., Wiegmann, A., & Zhan, X. (2013). Digital rock physics benchmarks—Part I: Imaging and segmentation. *Computers & Geosciences*, **50**, 25–32. https://doi.org/10.1016/j.cageo.2012.09.005

Bazaikin, Y., Gurevich, B., Iglauer, S., Khachkova, T., Kolyukhin, D., Lebedev, M., Lisitsa, V., & Reshetova, G. (2017). Effect of CT image size and resolution on the accuracy of rock property estimates. *Journal of Geophysical Research: Solid Earth*, **122**(5), 3635–3647. https://doi.org/10.1002/2016jb013575

Chen, H., Zhang, Y., Zhang, W., Liao, P., Li, K., Zhou, J., & Wang, G. (2017). aLow-dose CT via convolutional neural network. *Biomedical Optics Express*, **8**(2), 679. https://doi.org/10.1364/boe.8.000679

Chung, T., Wang, Y. D., Armstrong, R. T., & Mostaghimi, P. (2019). Approximating Permeability of Microcomputed-Tomography Images Using Elliptic Flow Equations. *SPE Journal*, **24**(03), 1154–1163. https://doi.org/10.2118/191379-pa

Grubinger, M., P. Clough, H. Müller, and T. Deselaers. "The IAPR TC-12 Benchmark: A New Evaluation Resource for Visual Information Systems." Proceedings of the OntoImage 2006 Language Resources For Content-Based Image Retrieval. Genoa, Italy. Vol. **5**, May 2006, p. 10.

He, K., Zhang, X., Ren, S., & Sun, J. (2015, February 6). *Delving Deep into Rectifiers: Surpassing Human-Level Performance on ImageNet Classification*. ArXiv.Org. https://arxiv.org/abs/1502.01852

Kim, J., Lee, J. K., & Lee, K. M. (2015, November 14). *Accurate Image Super-Resolution Using Very Deep Convolutional Networks*. ArXiv.Org. https://arxiv.org/abs/1511.04587

Liu, T., Jin, X., & Wang, M. (2018). Critical Resolution and Sample Size of Digital Rock Analysis for Unconventional Reservoirs. *Energies*, **11**(7), 1798. https://doi.org/10.3390/en11071798

MathWorks. (n.d.-a). *Define Custom Regression Output Layer - MATLAB & Simulink*. Retrieved January 14, 2021, from https://www.mathworks.com/help/deeplearning/ug/define-custom-regression-output-layer.html

MathWorks. (n.d.-b). *Single Image Super-Resolution Using Deep Learning - MATLAB & Simulink Example*. Retrieved January 14, 2021, from https://www.mathworks.com/help/images/single-image-super-resolution-using-deep-learning.html

Pingel, J. (2019, February 21). Image-to-Image Regression. *Deep Learning*. https://blogs.mathworks.com/deep-learning/2019/02/21/image-to-image-regression/

Ronneberger, O., Fischer, P., & Brox, T. (2015, May 18). *U-Net: Convolutional Networks for Biomedical Image Segmentation*. ArXiv.Org https://arxiv.org/abs/1505.04597

Wang, Y. D., Armstrong, R. T., & Mostaghimi, P. (2019). Enhancing Resolution of Digital Rock Images with Super Resolution Convolutional Neural Networks. *Journal of Petroleum Science and Engineering*, **182**, 106261. https://doi.org/10.1016/j.petrol.2019.106261

Wang, Y. D., Armstrong, R. T., & Mostaghimi, P. (2020). Boosting Resolution and Recovering Texture of 2D and 3D Micro-CT Images with Deep Learning. *Water Resources Research*, **56**(1), 1. https://doi.org/10.1029/2019wr026052

Wildenschild, D., & Sheppard, A. P. (2013). X-ray imaging and analysis techniques for quantifying pore-scale structure and processes in subsurface porous medium systems. *Advances in Water Resources*, **51**, 217–246. https://doi.org/10.1016/j.advwatres.2012.07.018

Zhang, K., Zuo, W., Chen, Y., Meng, D., & Zhang, L. (2017). Beyond a Gaussian Denoiser: Residual Learning of Deep CNN for Image Denoising. *IEEE Transactions on Image Processing*, **26**(7), 3142–3155. https://doi.org/10.1109/tip.2017.2662206

Zhao, H., Gallo, O., Frosio, I., & Kautz, J. (2017). Loss Functions for Image Restoration With Neural Networks. *IEEE Transactions on Computational Imaging*, **3**(1), 47–57. https://doi.org/10.1109/tci.2016.2644865